Journal of
Ceramic Science
and Technology

J. Ceram. Sci. Tech., 07 [01] 97-106 (2016)
DOI: 10.4416/JCST2015-00040
available online at: http://www.ceramic-science.com

Influence of Titanium Silicide Active Filler on the Microstructure Evolution of Borosiloxane-Derived Si-B-O-C ceramics

V. Vijay[1], S. Bhuvaneswari[2], V. M. Biju[3], R. Devasia[*1]

[1]Ceramic Matrix Products Division, Vikram Sarabhai Space Centre,
Thiruvananthapuram 695022, Kerala, India
[2]Analytical and Spectroscopy Division, Vikram Sarabhai Space Centre,
Thiruvananthapuram 695022, Kerala, India
[3]Department of Chemistry, National Institute of Technology, Tiruchirappalli 620015, Tamil Nadu, India
received July 29, 2015; received in revised form September 4, 2015; accepted September 30, 2015

Abstract

Interactions between a typical polyborosiloxane containing methyl and vinyl functionalities, (BoSiVi) and active filler ($TiSi_2$) at 1500 °C under inert atmosphere were studied. The effects of filler content on the volume shrinkage, porosity, phase evolution and microstructure of the resulting ceramic were studied in detail. The optimum concentration of the active filler to fabricate Si-B-Ti-O-C ceramic with zero volume shrinkage was calculated. Pore size distribution uniformity in the resulting ceramic was increased with the incorporation of the filler into the polymer. XRD and Raman analyses confirm the evolution of TiC, TiOC, TiB_2, and SiC ceramics with stacking faults by active-filler-controlled polyborosiloxane pyrolysis. SEM-EDX, FESEM and HR-TEM analyses reveal the growth of ceramic nanofibres on the ceramic matrix as the result of a novel solution-precipitation process. Polyborosiloxane/active filler reactions are found to have a highly significant influence on the volume shrinkage, porosity, phase evolution, etc. of the final ceramic, which are critical parameters of an advanced structural material.

Keywords: Polyborosiloxanes, active filler controlled polymer pyrolysis (AFCOP), catalyst-assisted pyrolysis, ceramic nanofiber, titanium disilicide

I. Introduction

The preceramic polymer route for the synthesis of ceramics offers potential advantages over the conventional powder processing route, such as suitability for plastic shaping technology, high purity of the starting materials, formation of nanostructures or nano-domains and low processing temperatures [1]. Polymer-derived ceramics (PDC) are promising candidates for high-temperature applications owing to their low density, excellent oxidation resistance, near-zero creep behaviour and high thermal shock resistance [2–3]. The major limitation of the preceramic polymer route for bulk component fabrication is related to the tremendous volume shrinkage and crack formation during polymer to ceramic conversion.

Among the preceramic polymers, polyborosiloxanes are of particular interest because of their thermodynamically stable backbone linkages compared to siloxanes and the high ceramic yield [4]. Incorporation of heteroatoms like titanium, zirconium, hafnium, boron, etc. into a preceramic polymer increases the thermal stability of the resulting ceramic phase. Boron is also known to protect carbonaceous materials by forming a boron oxide film on the surface of the material [5]. Schiavon *et al.* and Packirisamy *et al.* have worked extensively on the synthesis of polyborosiloxanes and their conversion to ceramics [6–9]. On pyrolysis, polyborosiloxanes can yield mixed ceramics containing SiC, SiBOC and SiOC phases with high oxidation resistance owing to the formation of a protective layer of borosilicate glass. However, polyborosiloxanes are also associated with volume shrinkage and crack formation during the polymer to ceramic conversion. The volume shrinkage and crack formation increase the number of "Polymer Infiltration & Pyrolysis (PIP)" cycles during the fabrication of ceramic matrix composites. Introduction of inert fillers into the polyborosiloxanes is expected to reduce the volume shrinkage of the polymer during "polymer to ceramic conversion", thus reducing the macrocracks/pores and subsequently the number of PIP cycles.

Greil and co-workers have studied active fillers like titanium, silicon, molybdenum and chromium silicide with the polysiloxane and polycarbosilane system and coined the term Active-Filler-Controlled Polymer Pyrolysis (AFCOP) [10–15]. Active fillers react with the pyrolytic by-products of the preceramic polymer or with the reaction atmosphere, generating carbides, nitrides, oxides and silicides [11] resulting in "mixed ceramics" with enhanced oxidation resistance, electrical properties and mechanical properties. Previous reports have identified titanium silicide powder ($TiSi_2$, density = 4.01 g/cm^3) as an excellent active filler under nitridization and carburization atmosphere [12]. The specific volume change on carburization

* Corresponding author: d_renjith@vssc.gov.in

(147 vol%) and nitridization (153 vol%) of $TiSi_2$ active filler is very high compared to other reported active fillers. The nitridization behaviour of $TiSi_2$ is well established and $TiSi_2$-incorporated CMCs were also fabricated under the same atmosphere [16].

Taking into account the above mentioned facts, we have studied the effect of titanium silicide as an active filler during the pyrolysis of a typical polyborosiloxane. To the best of our knowledge, the effect of active filler on the pyrolysis of polyborosiloxane in an inert atmosphere has not been investigated. The effects of filler content on the volume shrinkage, porosity, phase evolution and microstructure of the resulting ceramics were studied in detail.

II. Materials and Methods

(1) Synthesis of polyborosiloxane (BoSiVi)

The polyborosiloxane (BoSiVi) used in the current investigation contained methyl and vinyl functional groups with a ceramic residue of ≈ 66 – 68 wt% at 1500 °C in argon atmosphere. BoSiVi was synthesized in a novel solventless process by reacting boric acid, methyl triethoxysilane and vinyl triethoxysilane as reported earlier [17–19]. The as-synthesized BoSiVi was a liquid oligomer, which was dried at 200 °C to obtain fine free-flowing BoSiVi powder. The empirical formula of BoSiVi is $C_{0.40}H_{1.0}Si_{0.30}B_{0.06}O_{0.66}$.

(2) Preparation of [BoSiVi + $TiSi_2$] pellets

BoSiVi powders were mixed with different percentage per weight (5, 10, 15, 20, 25 and 30) of titanium silicide ($TiSi_2$, M/s. Alfa Aesar, GmbH, purity = 99.5 %) with an average particle size of 30 μm. For effective mixing, both BoSiVi & $TiSi_2$ powders were dispersed in ethanol followed by ultrasonication for 30 min. Ethanol was removed from the dispersion by means of evaporation and the well-dispersed mixtures were moulded to "green compacts" at room temperature under a pressure of 20 MPa. These green compacts were pyrolyzed in a tubular furnace under argon atmosphere (with a flow rate of 3 slpm) at a heating rate of 3 K/min. The tubular furnace was maintained at 1500 °C for 3 h followed by a programmed cooling to room temperature under argon atmosphere.

III Characterization techniques

The elemental composition of carbon and hydrogen was analysed using a Perkin Elmer Elemental Analyzer (Model PE 2400). The silicon composition in the sample was analysed using sodium carbonate fusion followed by ignition with perchloric acid and volatilization with hydrofluoric acid. The composition of boron in the sample was also estimated using sodium carbonate fusion followed by mannitol titration. The titanium composition was calculated by converting the sample to Ti-H_2O_2 complex (yellow colour) followed by an UV absorption study.

The bulk densities and true densities of [BoSiVi + $TiSi_2$] ceramics were measured according to the Archimedes principle (ASTM standard C20 – 92) and with He pycnometry (AccuPyc II 1340, Micrometrics). The residual porosity in the final ceramic specimens was assessed with regard to the bulk density and true density of the ceramic specimens. Thermal analysis (TG-DTA) measurements for BoSiVi and [BoSiVi + $TiSi_2$] systems were performed with TA Instruments®, SDT 2960 at 10 K/min under argon atmosphere (purity – 99.993 %, flow rate of 30 slpm). Differential scanning calorimetry (DSC) analysis was conducted in a Setaram® Labsys 1600 DSC machine at 10 K/min under argon atmosphere (purity – 99.993 %, flow rate of 30 slpm). The porosity of the samples was determined using a Quantachrome Pormaster® mercury porosimeter in the pressure range of 1.045 – 50.037 PSIA.

X-ray diffraction data (XRD, Bruker® D8-Advance) were collected using CuKα radiation (40 kV, 40 mA; step scan of 0.051, counting time of 5 s/step and λ = 1.54060 Å). Raman spectra were recorded with a WITec® alpha 300R Confocal Raman microscope using a frequency-doubled Nd:YAG laser of excitation wavelength 532 nm. Finely powdered samples were prepared for analysis, using a low-power laser (5 %). The morphological features of the samples were analyzed by means of scanning electron microscope (JEOL, JSM-6390LV), field emission scanning electron microscope (Carl Zeiss, Supra 55), and energy-dispersive X-ray spectroscope (JEOL, JED – 2300). High resolution transmission electron microscope (HRTEM, JEM-2100 operating at 300 kV) was used to observe the nanostructures evolved during the active-filler-controlled polyborosiloxane pyrolysis. TEM specimens were prepared by finely powdering the compacts into submicron-sized particles and dispersing these in acetone to form a uniform slurry. A drop of the slurry was transferred to a carbon-film-coated TEM grid.

IV. Results and Discussion

(1) Effect of $TiSi_2$ concentration on the physical properties of BoSiVi system

The polyborosiloxane (BoSiVi) used in the current investigation contained methyl and vinyl functional groups. BoSiVi was used as a preceramic matrix resin for the fabrication of ceramic-matrix composites by means of the polymer infiltration pyrolysis process (PIP), owing to its moderately high ceramic residue (≅ 66 – 68 wt% at 1200 °C in argon atmosphere) and good infiltration ability. Boron is expected to form a boron oxide film on the surface of the material and thus increase the thermal stability of the resulting ceramic phase. However, the BoSiVi is also associated with the volume shrinkage and crack formation during the polymer to ceramic conversion. The influence of $TiSi_2$ active filler on the physical properties of BoSiVi compacts after pyrolysis was investigated. BoSiVi with different percentage per weight of $TiSi_2$ was designated as BoSiVi+$TiSi_2$-0, BoSiVi+$TiSi_2$-5, BoSiVi+$TiSi_2$-10, BoSiVi+$TiSi_2$-15, BoSiVi+$TiSi_2$-20, BoSiVi+$TiSi_2$-25 and BoSiVi+$TiSi_2$-30 respectively. Residual porosity and the empirical formula of all the ceramics are shown in Table 1.

Table 1: Effect of $TiSi_2$ on the volume shrinkage of the BoSiVi system and the elemental composition of the resulting ceramic.

Sl. No.	Specimen	Volume change (%)	Residual porosity (%)	Ceramic residue (%) at 1500°C	Empirical formula
1	BoSiVi + $TiSi_2$-0	-43.03	45.41	66.2	$Si_{0.54}B_{0.11}OC_{0.51}$
2	BoSiVi + $TiSi_2$-5	-26.51	38.36	82.44	$Si_{0.56}B_{0.11}OTi_{0.02}C_{0.51}$
3	BoSiVi + $TiSi_2$-10	-10.97	31.20	84.22	$Si_{0.6}B_{0.11}OTi_{0.05}C_{0.52}$
4	BoSiVi + $TiSi_2$-15	-1.99	23.01	85.10	$Si_{0.65}B_{0.11}OTi_{0.07}C_{0.53}$
6	BoSiVi + $TiSi_2$-20	+ 10.52	18.51	86.25	$Si_{0.7}B_{0.1}OTi_{0.11}C_{0.53}$
7	BoSiVi+$TiSi_2$-25	+ 11.59	16.00	90.00	$Si_{0.74}B_{0.1}OTi_{0.15}C_{0.51}$
8	BoSiVi+$TiSi_2$-30	EXFOLIATED			$Si_{0.81}B_{0.1}OTi_{0.2}C_{0.52}$

The densities of the BoSiVi and [BoSiVi + $TiSi_2$] systems were calculated. This was followed by pyrolysis of the BoSiVi and [BoSiVi + $TiSi_2$] compacts at 1500 °C under argon atmosphere. The BoSiVi and [BoSiVi + $TiSi_2$] compacts were weighed and their densities and elemental composition estimated, followed by the evaluation of the volume change of the compacts on ceramic conversion. Variation of volume of the BoSiVi and [BoSiVi + $TiSi_2$] compacts is shown in Fig. 1.

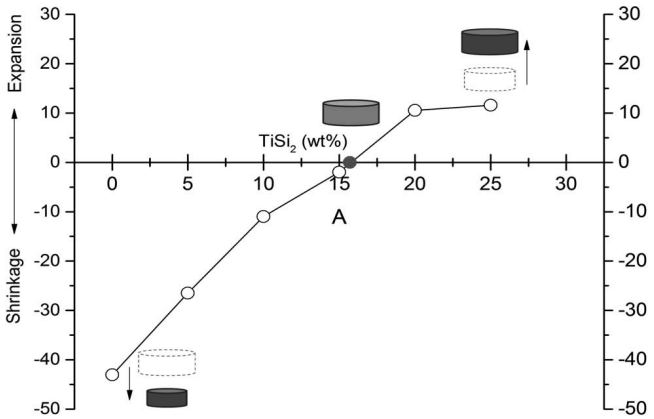

Fig. 1: Variation of volume shrinkage (%) of BoSiVi and [BoSiVi + $TiSi_2$] with the percentage per weight of $TiSi_2$.

In the case of BoSiVi+$TiSi_2$-0, volume shrinkage was 43.03 % and the resultant ceramic was extremely brittle. As the $TiSi_2$ filler loading increases (5, 10 and 15 wt%), the corresponding volume shrinkage decreases up to 1.99 % whereas in the case of BoSiVi+$TiSi_2$-20 and BoSiVi+$TiSi_2$-25 a resultant volume expansion was noticed. But the BoSiVi+$TiSi_2$-30 system was exfoliated after pyrolysis at 1500 °C. This may be due to the fact that the quantum of volume expansion of the filler exceeds the volume shrinkage of the polymer on pyrolysis. The concentration of $TiSi_2$ required for "zero volume shrinkage" of the BoSiVi system on polymer to ceramic conversion was estimated from the point at which the line intersects the X-axis as 15.6 wt%.

The ceramic residue of BoSiVi and [BoSiVi + $TiSi_2$] systems at 1200 °C under argon atmosphere is represented in Fig. 2. BoSiVi+$TiSi_2$-0 returns a ceramic yield of ≈ 82 % at 1200 °C and as the filler loading increases, the ceramic residue of the system also increases up to ≈ 90 %. The increase in ceramic residue may be attributed to the increase in the non-volatile filler content as well as the pyrolytic reaction by-products of the polymer and the active filler.

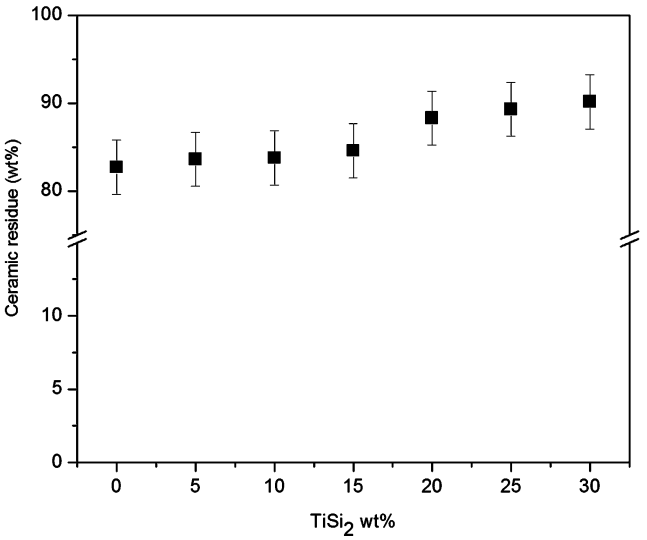

Fig. 2: Variation of ceramic residue (wt%) of the BoSiVi and [BoSiVi + $TiSi_2$] systems with the percentage per weight of $TiSi_2$ (1200 °C in argon atmosphere, f = 10 K/min)

To determine the temperature regime of the reaction between $TiSi_2$ and BoSiVi, differential scanning calorimetric (DSC) analysis was performed. The DSC curve of the BoSiVi+$TiSi_2$-0 and BoSiVi+$TiSi_2$-30 green compacts is shown in Fig. 3.

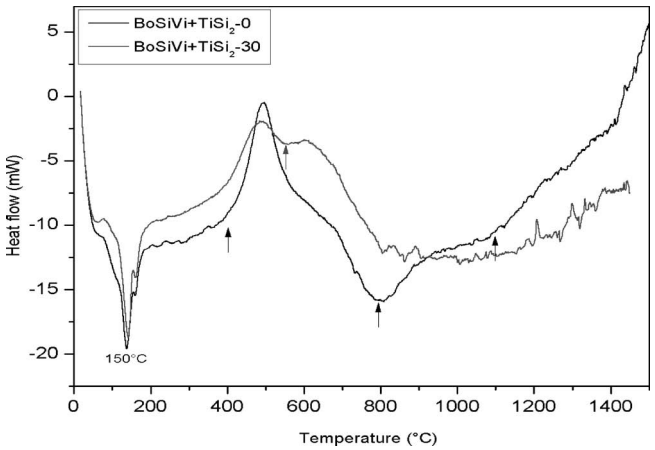

Fig. 3: DSC curves of (a) BoSiVi+$TiSi_2$-0 (b) BoSiVi+$TiSi_2$-30.

The green compacts exhibited an endothermic peak at ≈ 150 °C, associated with the release of boric acid as reported by previous authors [20]. BoSiVi+$TiSi_2$-0 exhibited an exothermic peak at ≈ 400 – 800 °C, which was attributed to the polymer to ceramic conversion. At this temperature regime, hydrocarbons were released from the system owing to complex rearrangement of the polymer to ceramic, and as a result the formation of a ceramic matrix with transient porosity was initiated. Schiavon *et al.* [21] reported that polysiloxanes in the temperature regime of ≈ 400 – 800 °C represent a random distribution of SiO_4, SiO_3C, SiO_2C_2, $SiOC_3$ and SiC_4 moieties. The DSC curve of BoSiVi+$TiSi_2$-30 system clearly shows a deviation at a temperature of ≈ 550 °C. This may be due to the initiation of reaction of $TiSi_2$ filler with the pyrolytic products of the polymer, which implies that the active filler starts reacting from ≈ 550 °C.

The porosity generated in the pyrolyzed BoSiVi and [BoSiVi + $TiSi_2$] systems was evaluated by means of mercury porosimetry. The average pore diameter and pore volume distribution of BoSiVi+$TiSi_2$-0, BoSiVi+$TiSi_2$-15 and BoSiVi+$TiSi_2$-25 systems were analysed. Fig. 4 indicates that as the filler percentage per weight increases, the peak of the *"average pore diameter"* is shifted towards a *"lower diameter regime"*, indicating that the average pore diameter decreases with an increase in filler loading. The average pore diameter of BoSiVi+$TiSi_2$-0, BoSiVi+$TiSi_2$-15 and BoSiVi+$TiSi_2$-25 was 82 μm, 69 μm and 66 μm respectively.

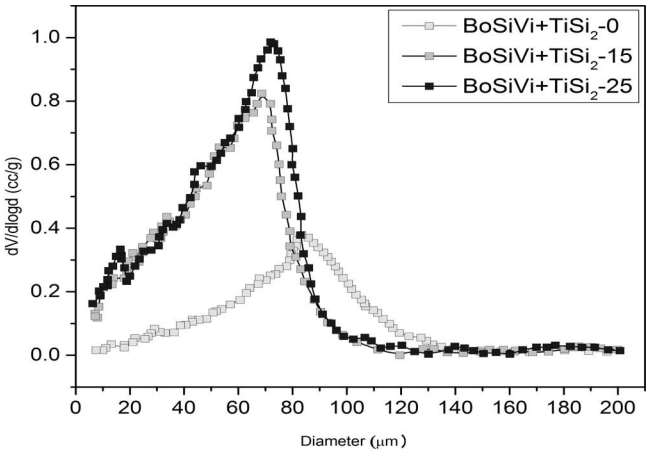

Fig. 4: Porosity distribution curves of typical BoSiVi and [BoSiVi + $TiSi_2$] systems heat-treated at 1500 °C.

It was also observed that with the addition of $TiSi_2$ filler, the pore size distribution in the ceramic samples became more uniform and the peaks became narrower compared to that of BoSiVi-derived ceramic phase.

(2) Effect of $TiSi_2$ concentration on the phase evolution of BoSiVi system

X-ray diffraction studies were performed to investigate the evolution of ceramic phases in BoSiVi and [BoSiVi + $TiSi_2$] systems. Initially, the XRD pattern [Fig. 5(A)] of $TiSi_2$ active filler was evaluated (before and after heat treatment at 1500 °C), which shows the presence of titanium, silicon, carbon as impurities along with $TiSi_2$ phase. Fig. 5(B) gives the XRD pattern of $TiSi_2$ after heat treatment at 1500 °C, showing the evolution of TiC and SiC phases. XRD patterns corresponding to excess titanium and carbon disappeared after the heat treatment at 1500 °C. Carbon in the system may react with $TiSi_2$, Ti and Si to form corresponding carbides. However, even after the heat treatment, trace amounts of silicon were present in the filler material.

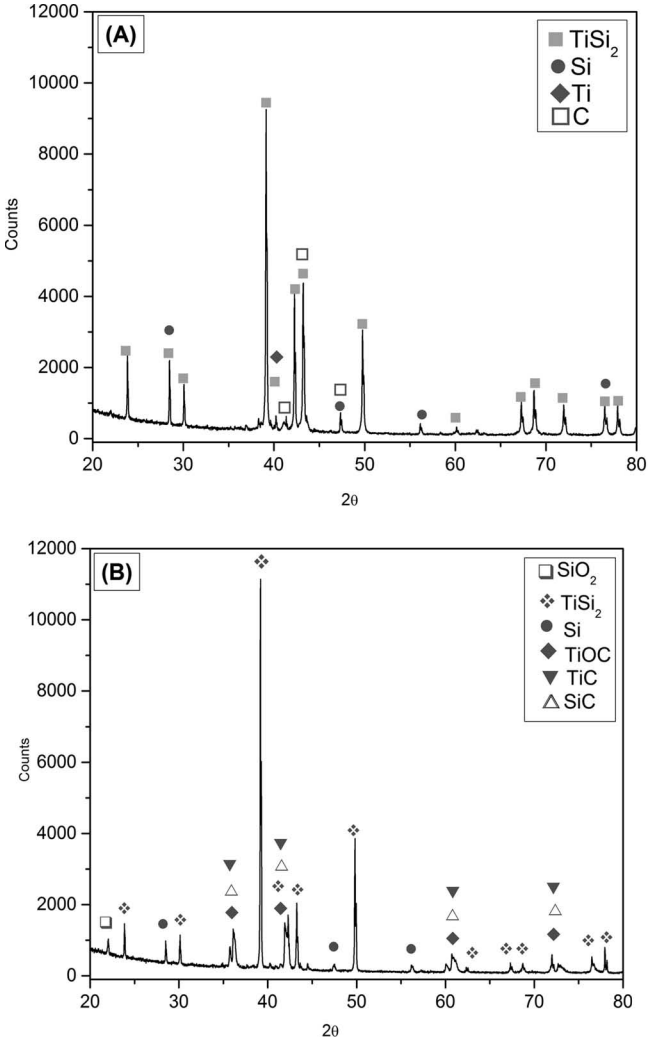

Fig. 5: XRD pattern of (A) as-received $TiSi_2$ (B) $TiSi_2$ heat-treated at 1500 °C.

Raman analysis of $TiSi_2$ before and after pyrolysis at 1500 °C was also performed to co-relate with the XRD spectral data. As the phase evolutions in ceramic materials were non-homogeneous, Raman analysis were recorded from different spots/areas of the powdered samples, as indicated in Fig. 6. The conclusions from the XRD spectra were proved correct as TiC_xO_y phases were identified (broad peaks centred at ≈ 400 and 600 cm^{-1}) in the Raman spectrum of $TiSi_2$ heat-treated at 1500 °C.

The peaks at ≈ 421 and 605 cm^{-1} were attributed to the existence of non-stoichiometric TiC [23]. $TiSi_2$ exhibits a broad peak at 303 cm^{-1} but as the system contains TiC and TiC_xO_y and these exhibit broad bands in the same region there are chances of peak overlapping. The peak centred at ≈ 280 cm^{-1} confirms the presence of SiO_2. Characteristic peaks of SiO_2 at ≈ 420 cm^{-1}, 520 cm^{-1} and 800 cm^{-1} may also overlap with the peaks of TiC and SiC phase in the system. Broad peaks at ≈ 1334 and 1550 cm^{-1} indicate the

presence of amorphous carbon in the system. The sharp and intense peak centred at ≈ 775 cm^{-1} confirms the presence of SiC involving random or periodic stacking faults of the planes along the (111) cubic or (001) hexagonal direction [24].

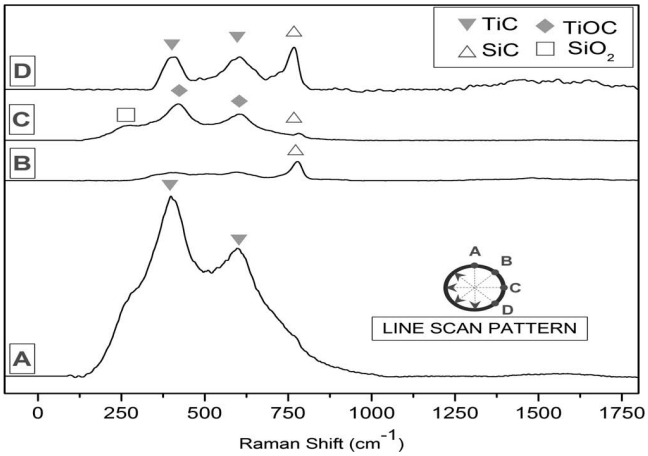

Fig. 6: Raman spectra of $TiSi_2$ heat-treated at 1500 °C.

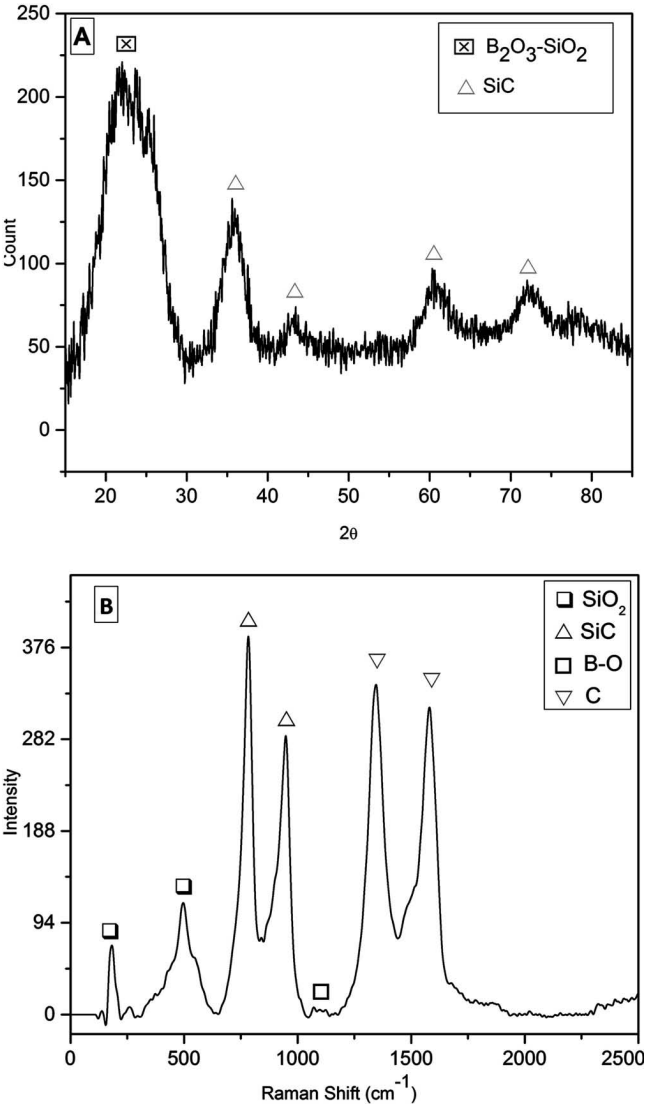

Fig. 7: (A) XRD pattern and (B) Raman spectrum of BoSiVi heat treated at 1500 °C.

XRD pattern and Raman spectrum of BoSiVi + $TiSi_2$-0 system after heat treatment at 1500 °C are shown in Fig. 7(A) and 7(B) respectively. The XRD spectra show the evolution of characteristic peaks of β-SiC along with a broad pattern at 2θ ≈ 22° which indicates the formation of B_2O_3-SiO_2 (JCPDS#00 – 042 – 0383). The Raman spectrum also complements the XRD data where characteristic peaks of β-SiC are observed. The characteristic β-SiC peaks observed in the Raman spectrum at ≈ 784, 949 cm^{-1} imply that it is devoid of any stacking faults [25].

In order to determine the effect of filler concentration on the phase evolution, the XRD pattern of BoSiVi was compared with the spectra of the [BoSiVi + $TiSi_2$] systems pyrolyzed at 1500 °C (Fig. 8).

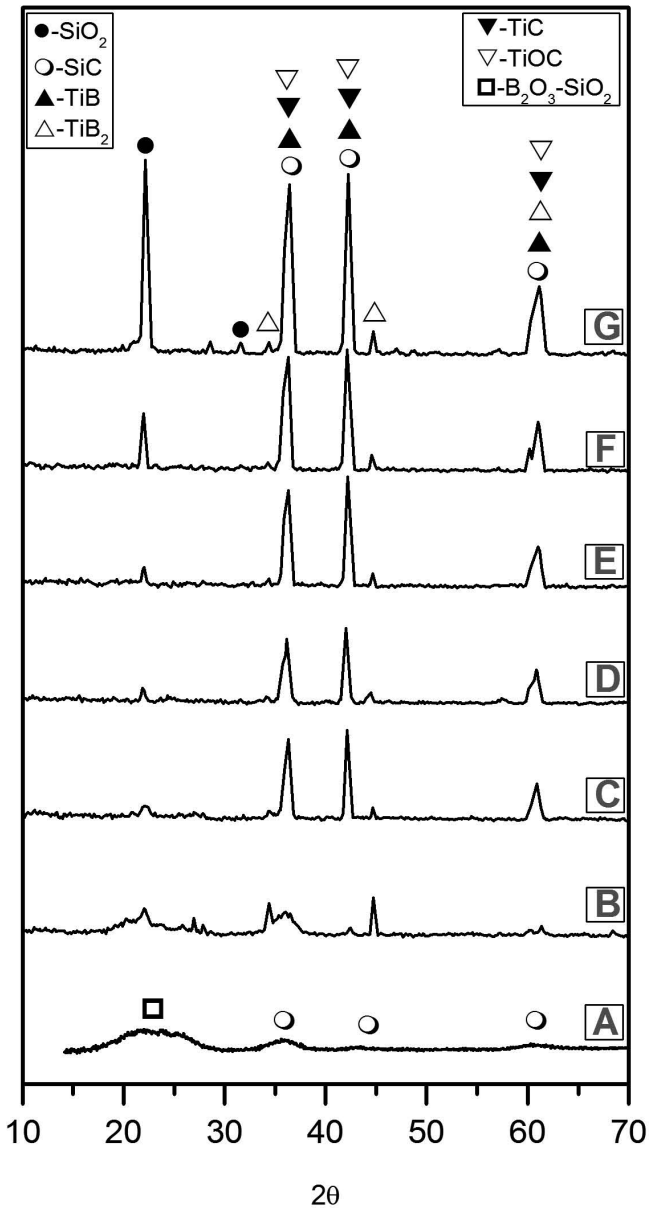

Fig. 8: XRD pattern of (A) BoSiVi+$TiSi_2$-0, (B) BoSiVi+$TiSi_2$-5, (C) BoSiVi+$TiSi_2$-10, (D) BoSiVi+$TiSi_2$-15, (E) BoSiVi+$TiSi_2$-20, (F) BoSiVi+$TiSi_2$-25 and (G) BoSiVi+$TiSi_2$-30 heat-treated at 1500 °C.

XRD patterns of [BoSiVi + $TiSi_2$] systems show the evolution of phases like TiB (JCPDS #04 – 004 – 9040) and TiB_2 (JCPDS#00 – 007 – 0275) in addition to SiC (JCPDS#04 – 002 – 9070), SiO_2 (JCPDS#04 – 007 – 2134), TiC (JCPDS#00 – 001 – 1222) and TiOC (JCPDS #04 – 006 – 1697) phases. Titanium borides may be formed owing to the reaction between boron in the poly-

borosiloxane and $TiSi_2$. As the filler concentration increases, the crystalline nature of the system also increases. It is evident from our study that the filler-incorporated polymer system at 1500 °C provides a mixture of oxide phases (SiO_2, TiOC and B_2O_3-SiO_2) and non-oxide ceramic phases (TiB_2, TiB and TiC).

Raman spectra of [BoSiVi + $TiSi_2$] systems heat-treated at 1500 °C complement the results obtained from XRD analysis. The SiC peak in the Raman spectra of [BoSiVi + $TiSi_2$] systems was situated at around ≈ 776 cm^{-1} (Fig. 9).

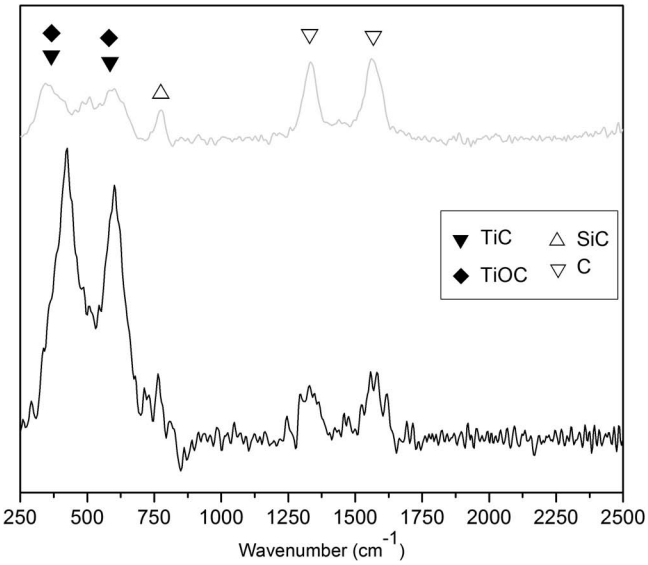

Fig. 9: Raman spectra of BoSiVi+$TiSi_2$ (30) heat-treated at 1500 °C.

The sharp and intense peak of SiC centred at ≈ 776 cm^{-1} is attributed to the coherent structure involving random or periodic stacking faults of the compact planes along the (111) cubic or (001) hexagonal direction. It was thus confirmed that the silicon carbide phase evolved from the $TiSi_2$-incorporated borosiloxane system does have periodic stacking faults. The Raman analysis technique could not detect the evolution of TiB_2 phase as it was Raman-inactive.

(3) Effect of $TiSi_2$ concentration on the morphological features of the BoSiVi system

The morphology of the BoSiVi and [BoSiVi + $TiSi_2$] systems was investigated using a scanning electron microscope equipped with energy-dispersive X-ray spectroscopy (SEM-EDX). From the SEM images of the cross-section of BoSiVi+$TiSi_2$-0 [Fig. 10(a)], it was observed that the system contains micropores.

Figs. 10(b) and 10(c) show the SEM images of cross-sections of BoSiVi+$TiSi_2$-15 and BoSiVi+$TiSi_2$-25 respectively. It is evident that the surface morphology of the BoSiVi+$TiSi_2$-15 system has more surface uniformity than the other two systems. Thus mercury porosimetry results and SEM images of the BoSiVi+$TiSi_2$ samples point towards the porosity-engineering capability of AFCOP. Accordingly, the pore size in the BoSiVi system can be tailored by changing the percentage per weight of $TiSi_2$ active filler in the system.

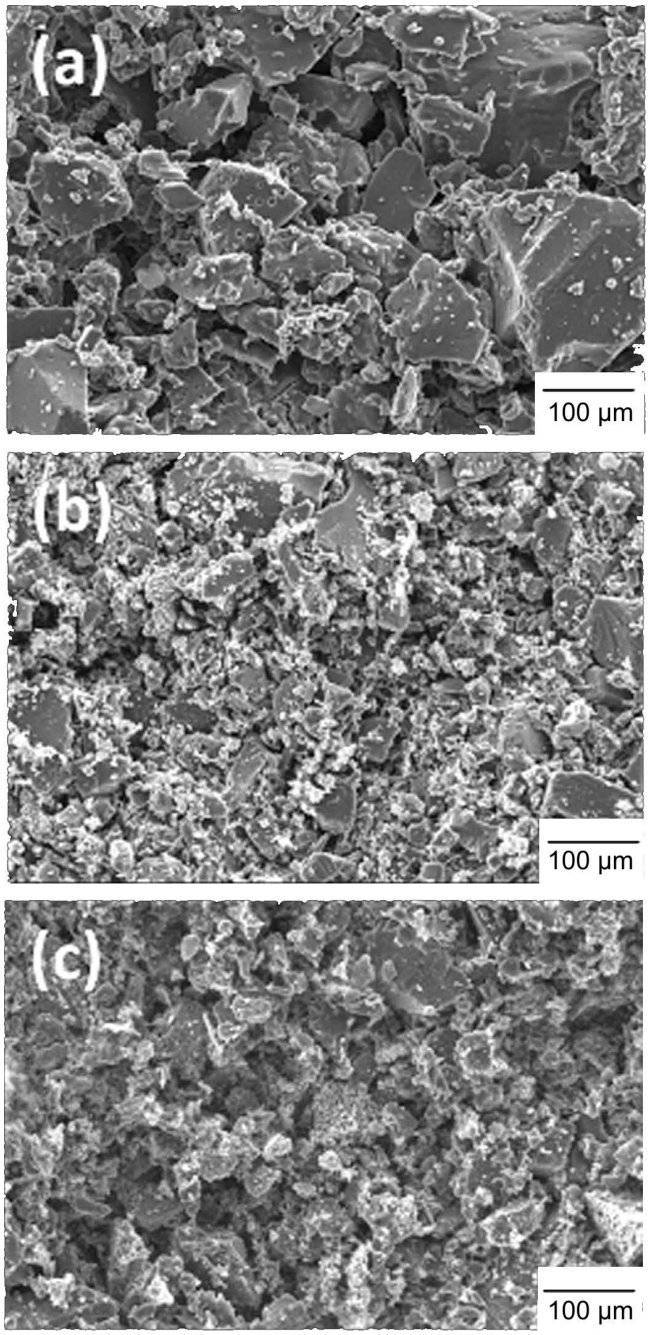

Fig. 10: SEM images of (a) BoSiVi+$TiSi_2$-0 (b) BoSiVi+$TiSi_2$-15 (c) BoSiVi+$TiSi_2$-25.

Fig. 11 shows higher-magnification SEM images of all the BoSiVi and [BoSiVi + $TiSi_2$] systems. SEM images of BoSiVi+$TiSi_2$-0 clearly indicate porosity in the matrix and EDX analysis confirms the presence of silicon, carbon and oxygen in the matrix.

The EDX composition analysis technique was used to identify the ceramic composition. Even though lighter elements can be detected, e.g. boron, sensitivity to them is low, thus making quantification difficult. However, chemical analysis of pyrolyzed products confirms the presence of ≤ 3 wt% of boron in the ceramic phase. The presence of borides in the ceramic phases was also identified from XRD analysis.

In the case of BoSiVi+$TiSi_2$-5, nanogrowth was observed and the concentration of the nanogrowth was found to increase as the concentration of the filler increases. Field

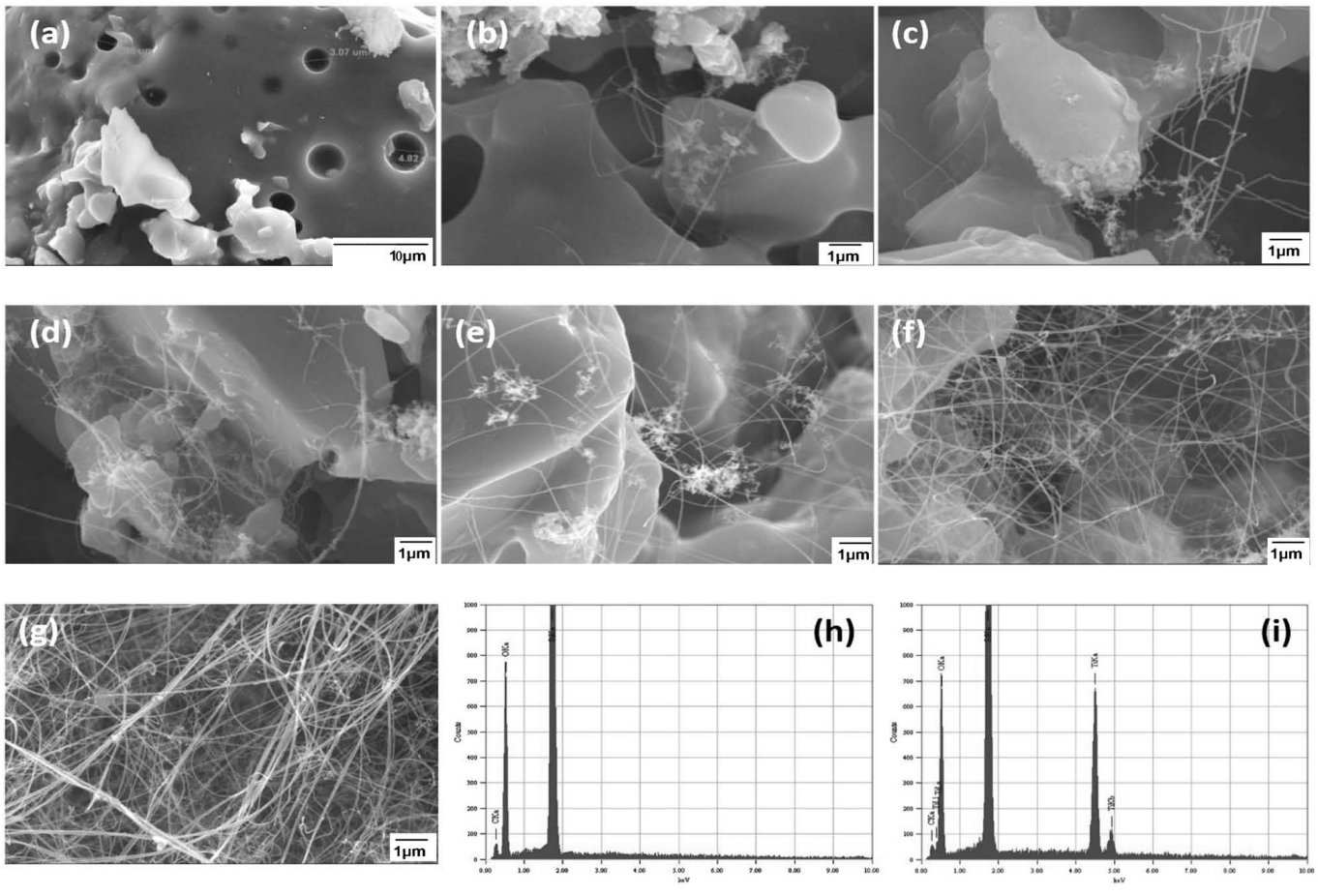

Fig. 11: SEM images of (A) BoSiVi+$TiSi_2$-0, (B) BoSiVi+$TiSi_2$-5, (C) BoSiVi+$TiSi_2$-10, (D) BoSiVi+$TiSi_2$-15, (E) BoSiVi+$TiSi_2$-20, (F) BoSiVi+$TiSi_2$-25 and (G) BoSiVi+$TiSi_2$-30 and EDX mapping of (H) BoSiVi+$TiSi_2$ (0), (I) BoSiVi+$TiSi_2$ (30).

emission scanning electron microscopy (FESEM) images and EDX studies of BoSiVi+$TiSi_2$-30 proved that the matrix was fully covered with nanofibres and the EDX mapping confirms the presence of silicon, carbon, oxygen and titanium. Growth of nanostructures via pyrolysis of transition-silicide-incorporated preceramic polymer is termed catalyst-assisted pyrolysis (CAP) [26].

In the above systems at low concentration of $TiSi_2$, nanogrowth was initiated in pores, which can be termed "catalytic micro-reactors" as reported by some authors [27]. From the present study it was observed that as the concentration of the catalyst increases catalytic-micro reactors were not required for the evolution of nanogrowth. As the concentration increases, the molten $TiSi_2$ filler material is no longer restricted to the micropores in the ceramic matrix but spreads over the matrix, and hence catalytic micro-reactors are not a prerequisite for the growth of ceramic nanofibres.

From the FESEM images (Fig. 12), it was observed that every nanowire contains a spherical tip and EDX analysis confirms that this spherical tip contains $TiSi_2$ with some oxygen.

From the EDX analysis, it was confirmed that the middle part of the nanowire and the matrix was made up of TiC-doped SiOC phase (Fig. 12). The growth mechanism of these nanowires was explained based on the vapour-liquid-solid (VLS) mechanism [28]. $TiSi_2$ is a very good solvent for SiC because of its high apparent solubility and low vapour pressure compared to other transition metal silicides [29]. Formation of SiC phase in the system can be explained with the following reactions:

$$SiO_{(g)} + 3CO_{(g)} \rightarrow SiC_{(s)} + 2CO_{2\ (g)} \quad (1)$$

$$TiSi_{2\ (l)} + 2C^*_{(s)} \rightarrow TiC\ (O)_{\ (s)} + 2SiC\ (O)_{\ (s)} \quad (2)$$

$$SiO_{\ (g)} + 2C_{\ (s)} \rightarrow SiC_{(s)} + CO_{\ (g)} \quad (3)$$

$$SiO_{2\ (s)} + 2C_{\ (s)} \rightarrow SiC_{\ (s)} + CO_{2\ (g)} \quad (4)$$

* *With traces of oxygen from the borosiloxane matrix.*

Previous investigations show that, reaction (1), the gas-gas reaction is thermodynamically unfavourable [30] in the temperature regime of the present study. So the formation of SiC can be explained based on a liquid-solid phase reaction as per Eq. (2) and a gas-solid phase reaction as per Eq. (3). Instead of the silicon suboxide reaction for SiC formation, a solid-solid reaction may happen as per Eq. (4). Silica may react with free carbon in the system in the temperature regime of the present study.

To obtain a better insight into the morphology of the nanofibre, an HRTEM image (Fig. 13) was recorded. The HRTEM image exhibits an array of planar defects on the nanofibre. Moreover, the nanofibre is surrounded by an amorphous layer comprising SiO_x phase. The thickness of the amorphous sheath is around 2 nm and that of the nanofibre is around 39 nm.

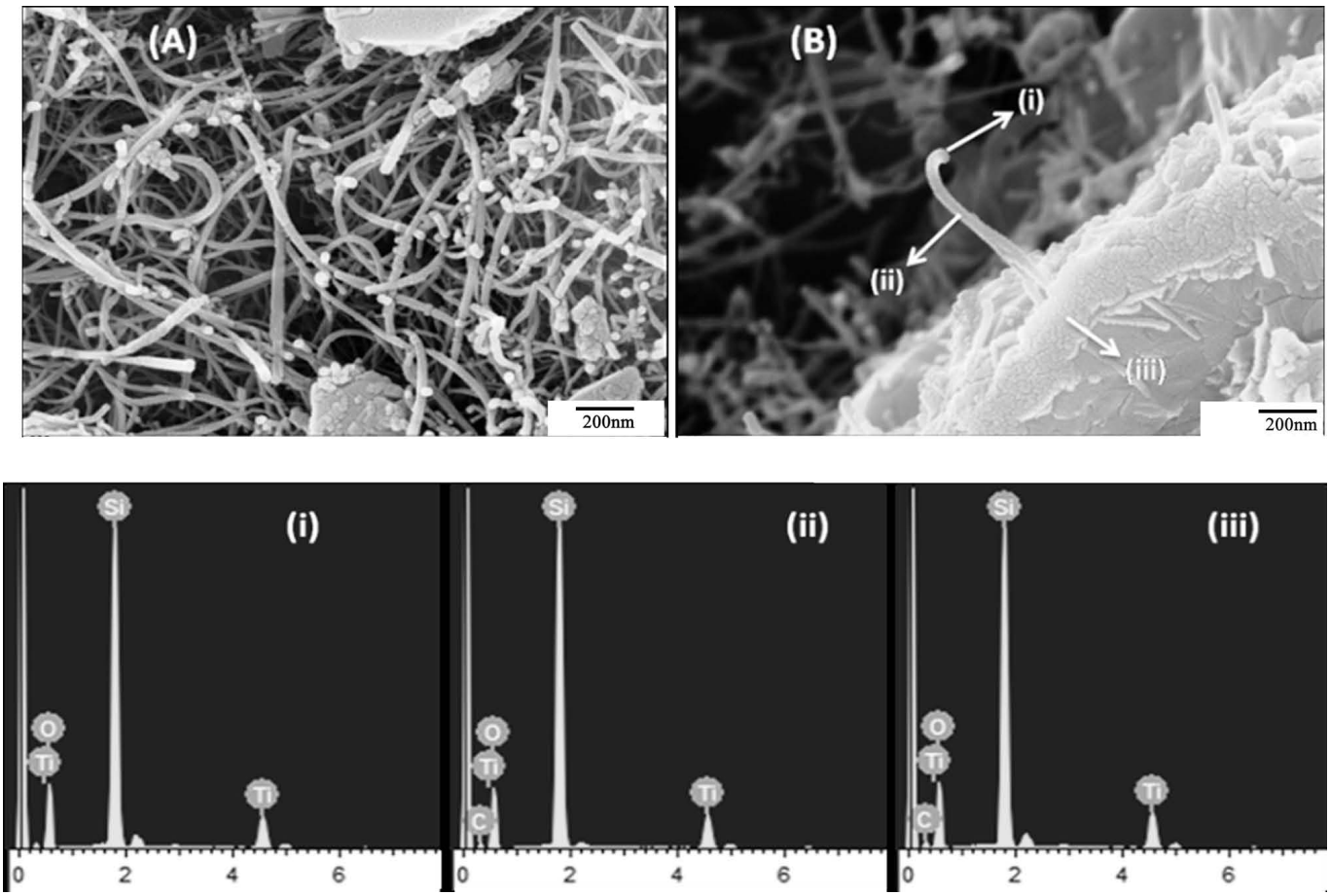

Fig. 12: FESEM image and related EDX spectra taken from selected areas of nanogrowth in BoSiVi+$TiSi_2$-30 (top: spherical tip; middle: nanowire; bottom: matrix phase).

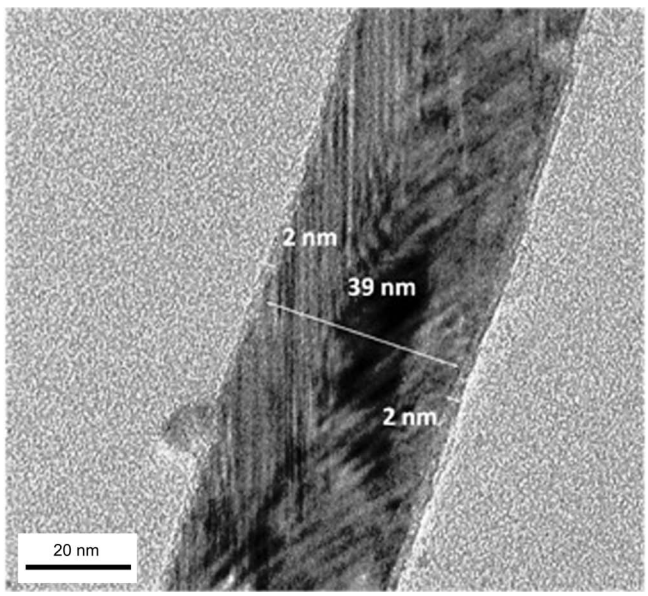

Fig. 13: HRTEM image of the Si-Ti-O-C nanofibre.

Owing to presence of excess oxygen in the preceramic system, the above products contain oxygen as an integral part. SiC dissolves in the molten $TiSi_2$ at high temperature to form a saturated solution of SiC in $TiSi_2$. Upon cooling, SiC phase crystallizes out with oxygen and some amount of TiC, in the form of nanowires from the solution. Hence the tip of the nanogrowth is observed to consist of Ti, Si and oxygen. Eq. (2) clearly indicates the reason for the increase in concentration of nanowires with the increase in concentration of $TiSi_2$. The stacking faults observed in the *"SiC phase derived from $TiSi_2$"* active-filler-incorporated borosiloxane pyrolysis provide clear evidence for the proposed mechanism of nanogrowth.

V. Conclusions

The influence of titanium silicide active filler on the microstructure of borosiloxane-derived Si-B-O-C ceramics was investigated. A detailed study on the physical and microstructure characteristics of the final ceramic was conducted and the following conclusions were derived:

- From the present study, 15.6 wt% $TiSi_2$ active filler was found to be the optimum concentration to obtain a "shrinkage-free ceramic" from BoSiVi polymer at 1500 °C. Addition of excess $TiSi_2$ beyond the optimum concentration resulted in a volume expansion.
- BoSiVi+$TiSi_2$ ceramic phase systems exhibit uniform pore size distribution, reduced porosity and pore diameter compared to that of the ceramic phase from the filler-free polyborosiloxane system. Thus active-filler-controlled polyborosiloxane pyrolysis can be used to fabricate near-net-shaped ceramic components.

- The BoSiVi system exhibited the evolution of SiC phase without any stacking faults but the BoSiVi+$TiSi_2$ systems exhibited the evolution of SiC phase with stacking faults. The existence of stacking faults in the SiC phase is direct evidence for the evolution of phases as a result of active-filler-controlled polymer pyrolysis.
- SEM-EDX, FESEM and HRTEM analysis revealed nanogrowth evolution in the BoSiVi+$TiSi_2$ systems as a result of catalyst-assisted pyrolysis. The investigations ascertained that the growth of the nanostructures in the filler loaded system was based on a solution-precipitation mechanism. Thus ceramic nanofibres could be fabricated on a ceramic substrate by means of a simple heat treatment process.

It was concluded that addition of an optimum percentage per weight of $TiSi_2$ active filler during polyborosiloxane pyrolysis resulted in a "shrinkage-free" multi-component ceramic matrix consisting of TiC, SiC, TiB_2, SiO_2 and Ti-OC phases.

References

1 Bernard, S., Fiaty, K., Cornu, D., Miele, P., Laurent, P.: Kinetic modeling of the polymer-derived ceramics route: investigation of the thermal decomposition kinetics of poly [β(methylamino)borazine] precursors into boron nitride, *J. Phys. Chem. B.,* **110**, 9048 – 9060, (2006).

2 Blum, Y.D., Macqueen, D.B., Kleebe, H.J.: Synthesis and characterization of carbon-enriched silicon oxycarbides, *J. Eur. Ceram. Soc.,* **25**, 143 – 149, (2005).

3 Naslain, R.: Design preparation and properties of non-oxide CMCs for application in engines and nuclear reactors: an overview, *Comp. Sci. Tech.,* **64**, 155 – 170, (2004).

4 Siqueira, R.L., Yoshida, I.V.P., Pardini, L.C., Schiavon, M.A.: Poly(borosiloxanes) as precursors for carbon fiber ceramic matrix composites, *Mater. Res.*, **10**, 147 – 151, (2007).

5 Vijay, V., Prabhakaran, P.V., Devasia, R.: Processing and properties of SiC_f/SiBOC ceramic matrix composites by polyborosiloxane impregnation and pyrolysis. In: Proceedings of Carbon Materials 2012 (CCM12) Conference. BARC, Mumbai, 2013.

6 Siqueira, R.L., Pardini, L.C., Yoshida, I.V.P., Schiavon, M.A.: The protective role of poly(borosiloxanes)-derived ceramics in carbon fiber composite, *Mater. Sci. Forum*, **587**, 182 – 186, (2008).

7 Schiavon, M.A., Armelin, N.A., Yoshida, I.V.P.: Novel poly(borosiloxane) precursors to amorphous SiBCO ceramics, *Mater. Chem. Phys*., **112**, 1047 – 1054, (2008).

8 Sreejith, K.J., Packirisamy, S.: Phenylborosiloxane-derived ceramic matrix composites. In: Proceedings of High Temperature Ceramic Materials and Composites. Berlin, 2010.

9 Swaminathan, S., Painuly, A., Manwatkar, S.K., Packirisamy, S.: Preceramic polymer derived C/C-SiC and C/C-SiBCO composites for high temperature applications. In: Proceedings of High Temperature Ceramic Materials and Composites. Berlin, 2010.

10 Greil, P., Seibold, M.: Modeling of dimensional changes during polymer-ceramic conversion for bulk component fabrication, *J. Mater. Sci.,* **27**, 1053 – 1060, (1992).

11 Greil, P.: Active filler controlled polymer pyrolysis, *J. Am. Ceram. Soc.,* **76**, 207 – 213, (1993).

12 Cordelair, J., Greil, P.: Electrical characterization of polymethylsiloxane/$MoSi_2$-derived composite ceramics, *J. Am. Ceram. Soc.,* **84**, 2256 – 2259, (2001).

13 Greil, P.: Net shape manufacturing of polymer derived ceramics, *J. Eur. Ceram. Soc.,* **18**, 1905 – 1914, (1998).

14 Dernovsek, O., Bressiani, J.C., Bressiani, A.H.A., Acchar, W., Greil, P.: Reaction bonded niobium carbide ceramics from polymer-filler mixtures, *J. Mater. Sci.,* **35**, 2201 – 2207, (2000).

15 Kaindl, A., Lehner, W., Greil, P., Kim, D.J.: Polymer-filler derived Mo_2C ceramics, *Mater. Sci. Eng. A,* **260**, 101 – 107, (1999).

16 Maillé, L., Le Ber, S., Dourges, M.A., Pailler, R., Guette, A., Roger, J.: Manufacturing of ceramic matrix composite using a hybrid process combining $TiSi_2$ active filler infiltration and preceramic impregnation and pyrolysis, *J. Eur. Ceram. Soc.,* **34**, 189 – 195, (2014).

17 Sreejith, K.J.: Polymer derived ceramics and their high temperature applications. PhD thesis, University of Kerala, 2011.

18 Packirisamy, S., Devapal, D., Prabhakaran, P.V., Sreejith, K.J., Paul, A., Painuly, A.: A process for solvent less synthesis of resinous borosiloxane oligomers as precursors for ceramics. Indian Patent Application 113/CHE/2010 (2010).

19 Devapal, D., Packirisamy, S., Sreejith, K.J., Ravindran, P.V., George, B.K.: Synthesis, characterization and ceramic conversion studies of borosiloxane oligomers from phenyltrialkoxysilanes, *J. Inorg. Organomet. P.,* **20**, 666 – 674, (2010).

20 Soraru, G.D., Campostrini, R., Maurina, S., Babonneau, F.: Gel precursor to silicon oxycarbide glasses with ultra high ceramic yield, *J. Am. Ceram. Soc.,* **80**, 999 – 1004, (1997).

21 Schiavon, M.A.: Crystallization behavior of novel silicon boron oxycarbide glasses, *J. Am. Ceram. Soc.,* **87**, 203 – 208, (2004).

22 Allahverdi, M., Cannon, W.R., Danforth, S.C.: Processing and properties of Blackglas™-Nextel™ 312 (BN) composites incorporating fillers, *J. Am. Ceram. Soc.,* **83**, 2929 – 2937, (2000).

23 Lohse, B.H., Calka, A., Wexler, D.: Raman spectroscopy as a tool to study TiC formation during controlled ball milling, *J. App. Phys.,* **97**, 114912 – 114917, (2005).

24 Chollon, G.: Structural and textural analysis of SiC-based and carbon CVD coatings by raman microspectroscopy, *Thin Solid Films,* **516**, 388 – 396, (2007).

25 Baek, Y., Ryu, Y.H., Yong, K.: Structural characterization of H-SiC nanowires synthesized by direct heating method, *Mater. Sci. Eng. C,* **26**, 805 – 808, (2006).

26 Jou, S., Hsu, C.K.: Preparation of carbon nanotubes from vacuum pyrolysis of polycarbosilane, *Mater. Sci. Eng. B,* **106**, 275 – 281, (2004).

27 Scheffler, M., Greil, P., Berger, A., Pippel, E., Woltersdorf, J.: Nickel-catalyzed *in situ* formation of carbon nanotubes and turbostratic carbon in polymer-derived ceramics, *Mater. Chem. Phys.,* **84**, 131 – 139, (2004).

28 Berger, A., Pippel, E., Woltersdorf, J., Scheffler, M., Cromme, P., Greil. P.: Nano-processes in polymer-derived Si-O-C ceramics: electron microscopic observations and reaction kinetics, *Phys. Stat. Solid. A,* **202**, 2277 – 2286, (2005).

29 Pellegrini, P.W., Feldman, J.M.: Liquid phase epitaxial growth of SiC from transition-metal silicide solvents, *J. Crys. Growth*, **27**, 320 – 324, (1974).

30 Weimer, A.W., Nilsen, K.J., Cochran, G.A., Roach, R.P.: Kinetics of carbothermal reduction synthesis of beta silicon carbide, *AIChEJ*, **39**, 493 – 503, (1993).